Available online at www.eccomasproceedia.org
Eccomas Proceedia SMART (2023) 465-476

ECCOMAS
Proceedia

X ECCOMAS Thematic Conference on Smart Structures and Materials
SMART 2023
D.A. Saravanos, A. Benjeddou, N. Chrysochoidis and T. Theodosiou (Eds)

DATA-DRIVEN INVERSE DESIGN OF RESONANT STRUCTURES FOR LOCALLY RESONANT METAMATERIALS

SANDER DEDONCKER*, CHRISTIAN DONNER†, BART VAN DAMME*

*Empa - Swiss Federal Laboratories for Materials Science and Technology
Laboratory for Acoustics/Noise Control
Überlandstrasse 129, 8600 Dübendorf, Switzerland
e-mail: bart.vandamme@empa.ch

†Swiss Data Science Center
Turnerstrasse 1, 8092 Zürich, Switzerland

Abstract. In the development of locally resonant metamaterials, resonator design plays a crucial role. This paper presents a novel design approach. Our method uses a conditional variational autoencoder to identify patterns between design variables and modal parameters and subsequently generate designs satisfying arbitrary criteria. Multiple modes – hence, metamaterial band gaps – can be specified simultaneously. An example of a resonator family with six geometric variables and two targeted modes is further elaborated. In this case, the method is able to generate several designs that closely approximate the prescribed modal characteristics.

Key words: Metamaterial, Vibration, Resonator, Generative Design

1 INTRODUCTION

In recent years, metamaterials have garnered much interest in several fields of engineering because of their extraordinary potential to break with traditional design goals [1]. By virtue of a carefully designed micro- or mesostructure, metamaterials display exotic macroscopic properties that do not exist in known bulk materials. In noise and vibration engineering, in particular, locally resonant metamaterials (LRMs) have come to the fore as a promising technology. By exploiting the phenomenon of resonance, LRMs are able to direct the energy present in acoustic waves and structural vibrations. This has many applications, ranging from energy harvesting to suppressing (particularly low-frequency) vibrations or acoustic noise [2].

Since LRMs consist of many small-scale resonators that are integrated into or onto a host structure, their properties are determined in the first place by those of the resonators. Similar resonators are assumed to produce similar properties – particularly, band gaps – even in dissimilar host structures [3]. By combining resonator types, multiple band gaps can even be created [4]. Therefore, we focus on the design of the resonators.

Machine-learning (ML) inverse design has gained attention in recent years, where the costly finite element (FE) analysis in the design pipeline is replaced by cheaper data-driven surrogate

Peer-review under responsibility of the organizing committee of SMART 2023.
doi: 10.7712/150123.9801.450548

models. Generative models such as variational autoencoders (VAEs) [5] or generative adversarial networks [6] have recently been used for the design of molecules and metamaterials [7, 8, 9]. While these design strategies still require optimization guided by some learned surrogate model, the on-demand design was also addressed [10, 11], i.e. the desired properties of the design are already provided to the model.

The present work aims to facilitate resonator (and LRM) design by applying generative ML methods. We aim for a LRM with multiple bandgaps, induced by a single resonant structure with desired dynamic properties. To find a suitable geometry, we propose a data-driven approach by which the resonator (inverse) design is handled automatically by an inexpensive surrogate model, that can generate designs based on pre-specified functional properties. Relative to more traditional design methods, such as topology optimization, this method is hence able to provide a large diversity of designs in a very short time.

The remainder of this paper discusses our approach as follows. In the first section, we lay out the elementary parts – a suitable representation of resonator dynamics as well as a VAE network – and show how they fit together in our method. In the next section, we consider a parametric family of resonators that complies with practical manufacturing constraints. Many designs are randomly sampled and converted to high-fidelity FE models, from which modal parameters are extracted. This input and output data is used to train the VAE model, that after training can provide designs with predefined resonant properties. We then assess the network performance and use it to find designs satisfying a predefined dynamic response. A few select designs are studied in detail, being integrated into a LRM model.

2 METHODS

2.1 Design and analysis of locally resonant metamaterials

In order to create an effective LRM, the motion between the resonators and the host should be strongly coupled and the resonator's dynamic mass should be large [3]. For this latter requirement, the resonating mass should be high and the tuning frequency needs to match the excitation frequency (i.e. that of the source), so the dynamic mass is strongly amplified.

For illustration, consider a mass-spring resonator with a weightless attachment point. The dynamic mass may be defined as the ratio of the force and the acceleration of the attachment point. For a system with mass m, stiffness k and natural pulsation $\omega_n = \sqrt{k/m}$, this becomes

$$m_{\text{dyn}}(\omega) = m\frac{\omega_n^2}{\omega_n^2 - \omega^2}, \tag{1}$$

highlighting the importance of both the (physical) mass and the tuning frequency.

More realistic approaches would treat resonators as three-dimensional continuous structures, with (in principle) infinitely many degrees of freedom. However, it is still possible to derive an equivalent model from the structure's modal parameters. This results in a parallel arrangement of mass-spring systems, each corresponding to one vibration mode, where a *modal effective mass* replaces the lumped mass [12]. The equivalent model is attractive for two reasons. First,

it is easier to interpret, since the analysis and conclusions for the basic mass-spring resonator (as discussed above) can be applied. Second, it allows direct comparisons of very different resonators, independent of their material or (interface) geometry.

The direction of the motion is of course also an important factor in three-dimensional space. Fortunately, this directionality can also be taken into account via the definition of the modal effective mass. We concentrate on beam-, and shell-like host structures – where flexural waves dominate – so we mainly consider transverse translations. From the resonator's perspective, we assume that this corresponds to vertical motion.

In order to assess resonator performance in the context of LRMs, the dispersion diagram of an actual material can be studied. Band gaps are expected around each resonator modes, where the width relates to the modal effective mass. In the experiments below, we present an example of a beam-type metamaterial. To construct dispersion curves, we use the method of Liu and Hussein, which is a transfer matrix approach analyzing the host-resonator unit cell [13].

2.2 Generative inverse design using machine learning

To mitigate computationally expensive FE analysis to find a suitable LRM design for given tuning frequencies and modal masses, we attempt to train a data-driven surrogate model, which is cheap to evaluate, but still sufficiently accurate. Here, we resort to a conditional variational autoencoder (cVAE). A variational autoencoder (VAE) [5] is a cyclic architecture, which has two parts: (i) an encoder, which maps parameterized designs to a probabilistic latent space, (ii) and a decoder, which provides the approximate inverse map from the latent space back to the design parameters. Typically, the encoder and decoder, are modeled by neural networks. Once the VAE is learned on some initial dataset, the user can generate new designs by sampling the latent space, and then projecting the samples back to the design space via the decoder. In the case of the conditional VAE [14], the user additionally provides desired properties for the design as input to the decoder. If the cVAE correctly learned relations between the requested parameters, the generated designs have properties, that are close to the requested ones, allowing for efficient design without any posthoc optimization. Here we use a recently developed cVAE framework [15] to demonstrate its effectiveness for targeted LRM design.

2.3 An inverse design approach for metamaterial resonators

While cVAEs are a powerful tool for a wide range of inverse design problems, certain limitations have to be taken into account. Most importantly, the neural network implementation assumes (implicitly) that the modeled quantities exist in vector spaces and are related by continuous functions. Seen from the perspective of resonator design, it is not so trivial to identify such quantities. For instance, mode shapes or reaction force vectors have arbitrary scale and orientation, and are therefore not directly suited. Fortunately, as we saw before, we can reduce the relevant dynamics to two positive scalar parameters (mass and frequency) per mode.

Still, there remains an issue. Because modal analysis is essentially an eigenvalue decomposition, we can assume that the outcome varies continuously with e.g. geometric dimensions.

However, different modes exist on different 'branches' of the decomposition. It can occur that, for one design, branch A has higher frequency than branch B, whereas for another design, it is the other way around. Because modes are typically ordered by frequency in the analysis, assigning modes to the continuous branches is generally not straightforward.

While addressing this problem fully is out of this work's scope, we try to mitigate effects by the following two-step selection procedure. We first pick the first two modes with the largest modal effective mass (in the vertical direction). Then we sort the selected modes by ascending frequency, e.g. the first mode is the mode with the lowest frequency among the 2 modes with the largest mass.

In summary, our proposed method will use a cVAE to create an invertible mapping between, on the one hand, design parameters such as geometry, and on the other, the frequencies and modal effective masses of the 'heaviest' modes. When generating designs, the user should make sure that their requests are physically realizable. This means respecting the ordering, but also the relations between the parameters. For example, specifying the frequency and mass of mode 1 limits the possible ranges for mode 2. Here, we specify the parameters for mode 1, and conditioned on these specifications we sample a multivariate Gaussian distribution mode 2. The Gaussian was previously fitted to the data the cVAE was trained on.

3 EXPERIMENTS

3.1 Resonator design

For the resonator design, we target frequencies on the order of 0.1 to 10 kHz. For the purposes of this study, we assume that the resonators can be manufactured using a small-scale powder bed fusion machine. The maximum and minimum feature sizes are assumed to be in the order of 100 mm and 1 mm. We assume that the fusion process results in a homogeneous and isotropic material with density 7750 kgm^{-3}, Young's modulus 193 Gpa and Poisson's ratio 0.3 (typical values for stainless steel).

With this in mind, we propose a resonator that consists of 2 intersecting bodies (figure 1). The first body is a solid cylinder, which is intended to provide a flat, stiff and invariant surface though which the resonator can be attached to the host. The cylinder has a radius of 10 mm, is aligned along the z-axis and extends between $z = -5$ mm and $z = 10$ mm. The second body is a parameterized spiral-shaped arm, which is intended to provide modal mass at relatively low frequencies. To construct the arm, we first define a parametric curve

$$\begin{cases} x = w_{sp}\left(\dfrac{(s_{sp}-1)}{2\pi n_{sp}}\alpha + 1\right)\cos\alpha \\ y = w_{sp}\left(\dfrac{(s_{sp}-1)}{2\pi n_{sp}}\alpha + 1\right)\sin\alpha \qquad 0 \leq \alpha \leq 2\pi n_{sp}, \\ z = \dfrac{h_{sp}}{2\pi n_{sp}}\alpha \end{cases} \tag{2}$$

where $w_{sp} = 5$ mm is the spiral 'width', h_{sp} is the spiral height, s_{sp} is the spiral scaling factor,

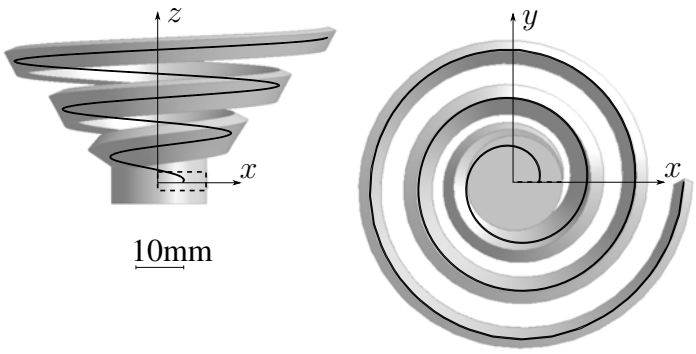

Figure 1: Geometry of the resonator. The spiral arm is constructed by sweeping a rectangle (dashed line) along a curve (solid line). The arm is partially embedded in a solid cylinder that is aligned with the spiral axis.

Table 1: Resonator design parameters with their bound constraints.

Parameter	Lower bound	Upper bound
Spiral height h_{sp}	0 mm	30 mm
Spiral scaling factor s_{sp}	2	8
Spiral number of turns n_{sp}	1	4
Cross-section width w_{cs}	2 mm	10 mm
Cross-section heigth h_{cs}	2 mm	4 mm
Cross-section scaling factor s_{cs}	0.5	2

and n_{sp} is the number of turns. A rectangle, centered on the spiral, is swept along the curve. At the start, this rectangle has width w_{cs} and height h_{cs} and is contained by the xz-plane. As the rectangle is extruded, its orientation relative to the curve is fixed, but its dimensions change linearly with the angle α. At the end of the curve, the rectangle becomes scaled by a factor s_{cs}.

We obtain a geometric family of resonators by independently varying the six free parameters (h_{sp}, w_{cs}, h_{cs}, s_{sp}, n_{sp} and s_{cs}). Considering the limitations of the manufacturing process, these parameters are bounded by the values in table 1. In addition, to prevent self-intersecting or oversized geometry, the following two constraints are imposed:

$$\begin{aligned} w_{cs}\max(s_{cs},1) &\leq w_{sp}\frac{s_{sp}-1}{n_{sp}} \\ w_{cs}\max(s_{cs},1) + 2w_{sp}s_{sp} &\leq 80\,\text{mm} \end{aligned} \tag{3}$$

3.2 Data generation

To train and test the ML approach, we create a data set by analyzing different resonators through a physics-based FE model. We first define a Latin hypercube sample on the input space,

with $n \gg 10000$ points. About half of these remain after discarding the designs violating the constraints. We randomly select 11000 points from this set, forming the input data set.

The designs are loaded into a commercial FE software (ANSYS [16]) which constructs the geometry, creates a mesh, and runs a preset modal analysis. In the analysis, the bottom face of the cylinder is subjected to a fixed boundary condition. The software calculates the twelve lowest-frequency eigenmodes. After the computation, the associated frequencies and (vertical) modal masses are written to disk. This evaluation process completes in most cases. However, because of various issues (mesh failures, licensing errors, etc.) certain designs fail to compute. Finally, 10513 complete data pairs could be obtained.

3.3 Network architecture and training

As mentioned before, the cVAE has two main building blocks. First, the variational encoder gets as input the design parameters, and its output is the mean and log variances of a Gaussian in the latent space. In addition, a simple surrogate forward model provides an estimate of the requested attributes. The second part, is the decoder taking a point in the latent space as input and the requested attributes and mapping these back to some design parameters. Both encoder and decoder are neural networks with two fully connected residual layers, each having 64 hidden units and a leaky ReLU as an activation function. Furthermore, we specify the latent space to be four-dimensional. We log-transform the performance attributes for the training to avoid negative frequencies and masses.

To train the network we need to minimize the losses for the different building blocks. For the encoder, these are the Kulback-Leibler divergence between the output Gaussian density and standard normal distribution. An additional loss is the mean squared error (MSE) between the true and the encoder's predicted performance attributes. The loss of the decoder is also the MSE between the design parameters of the training points and its predictions. 80% of the generated designs are used as training set, 10% are kept as validation set, and the remaining designs as test set. Then the cVAE is trained with mini-batches of 128 designs to minimize the total loss until no improvement is observed anymore on the validation training set.

4 RESULTS

After having trained the cVAE as described above, we first check the consistency of the model. To this end, we compute the design error on the held-out test set. The design error for feature i is defined as

$$\text{design error}_i = |y_i^{\text{pred}} - y_i^{\text{request}}|, \tag{4}$$

where y_i^{request} are the attributes the target design should have, and y_i^{pred} is the prediction of the cVAE's forward model for the designs suggested by its decoder. This can be considered as an approximate lower bound of errors to be expected. In figure 2 we see the average design errors for 1000 generated designs, and for the top 3 designs (those with the lowest summed design errors). In general, we observe, that the error of the top 3 designs is at least one order of magnitude lower than the requested value, meaning we can expect errors $< 10\%$. We also

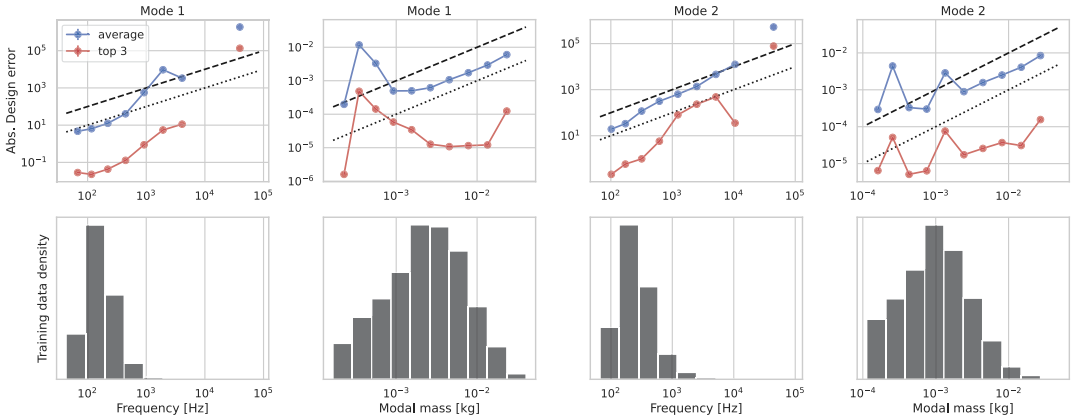

Figure 2: The predicted *design errors* for different performance attributes in the top panels. Blue line is the average over 1000 generated designs and red line indicates the error selecting the 3 designs with lowest error. Dashed line indicates identity (error is on the order of magnitude as request), and dotted line marks the line, where the error is one order of magnitude lower than the request. Lower panels display the histograms of the training data.

observe that errors increase for areas in the design space, where we provided less training data, emphasizing the importance of covering the desired design space well with the training data.

Next, we generate 1000 designs for 4 different requests and validate the top 20 in terms of design error by ANSYS, to check whether these result in designs that match well the requested LRM properties. In Figure 3 we visualize the top 3 designs of the 20 checked by ANSYS, and indeed we see a quite good match in general. However, when coming to the tails of the training distribution the results become less accurate, as we already have seen before in figure 2. Also, we observe that the requested attributes for mode 1 are matched more closely than those of the second mode.

Figure 4 and table 2 show the geometry and modal properties of some of the top-performing designs. Figures 4a-4b and 4c-4d are the cVAE's best proposals to satisfy, respectively, the first and second requests from table 2. These designs all give quite accurate approximations of the target parameters. It should not be a surprise that requesting lower frequencies generally leads to longer, more slender spirals. However, some design freedom remains. The cVAE appears to be effective in exploiting this, proposing geometrically distinct designs with highly similar modal parameters.

Thanks to the good approximation of modal parameters, the generated resonators also have the potential to produce band gaps that very accurately match those of the target. An example is given in figure 5, which shows the dispersion curves for a beam host structure. In this example, the beam has a rectangular cross-section with a (transverse) thickness of 2 mm and width of 125 mm. The shear correction factor is taken to be 5/6 and the material properties are the same as those of the resonators (section 3.1).

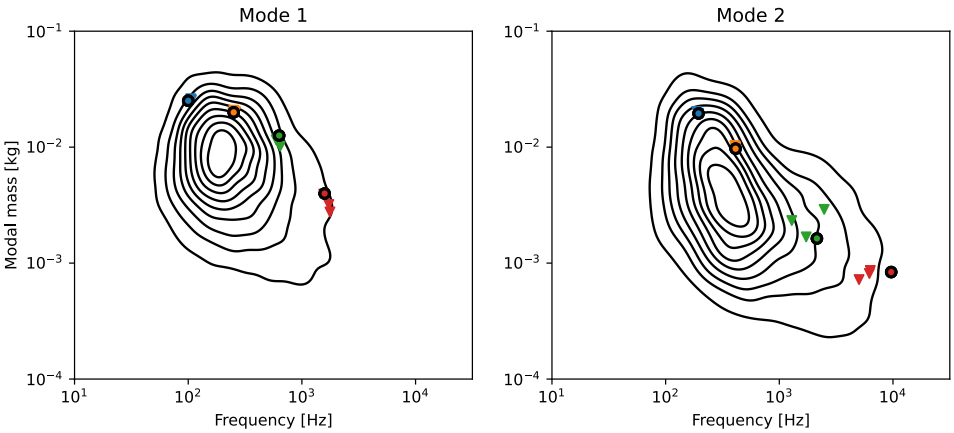

Figure 3: Requested attributes (circles) versus attributes of generated designs (triangles). The color indicates different requests. The contours indicate the training data for the cVAE.

Table 2: Targeted modal parameters and best approximating designs for two separate requests. Designs are ranked based on total relative error.

		Mode 1		**Mode 2**	
		Frequency [Hz]	Mass [g]	Frequency [Hz]	Mass [g]
Request 1	Target	100.0	25.12	194.8	19.51
	Design 1	104.8	25.99	194.0	19.60
	Design 2	105.8	26.05	194.0	19.26
Request 2	Target	251.2	19.95	412.5	9.693
	Design 1	260.8	20.19	412.4	9.797
	Design 2	251.7	20.80	413.5	10.08

(a) (b) (c) (d)

Figure 4: Resonator designs studied in detail. (a)-(b) Two best designs for the first request. (c)-(d) Two best designs for the second request.

5 CONCLUSION

In developing the next generation of acoustic materials, LRMs are a promising technology. LRM performance is largely determined by the resonator component. In this work, we propose and test a novel targeted design approach based on ML techniques. We argue that resonator designs can be evaluated mainly in terms of a few scalar modal parameters. After a tailored sorting procedure, these parameters can be used as performance attributes in a cVAE neural network. Consistency with the physical and mathematical properties of the data is thus enforced. After an offline training process – relying on numerical modal analyses for many designs – we obtain a fast (potentially interactive) method for resonator and hence LRM design. Multiple modes (forming multiple band gaps) can be requested simultaneously.

The approach is validated by applying it to a family of resonators that are spiral-shaped. The exact shape of the spiral is determined by six scalar parameters which form the design space. Around 10000 feasible designs are sampled and then analyzed using ANSYS, yielding the two modes with the largest effective mass for each design. A cVAE with relatively compact encoder and decoder networks is trained on this dataset. The dependencies between in- and outputs are shown to be captured very well in this manner. The cVAE predictions of modal parameters are in line with the 'true' values. The cVAE also proves capable of generating several different high-quality designs that match the target attributes exceptionally well. We finally show that this matching can translate to accurate band gap generation in a beam-type LRM.

Acknowledgements We express our gratitude to Luis Salamanca, Rafael Bischof, Aleksandra Anna Apolinarska, and Matthias Kohler for generously providing their code for the cVAE framework [15], which we trained the generative inverse design model with.

REFERENCES

[1] J. U. Surjadi, L. Gao, H. Du, X. Li, X. Xiong, N. X. Fang, and Y. Lu, "Mechanical Metamaterials and Their Engineering Applications," *Advanced Engineering Materials*, vol. 21, no. 3, p. 1800864, 3 2019. [Online]. Available: https://onlinelibrary.wiley.com/doi/full/10.1002/adem.201800864https:

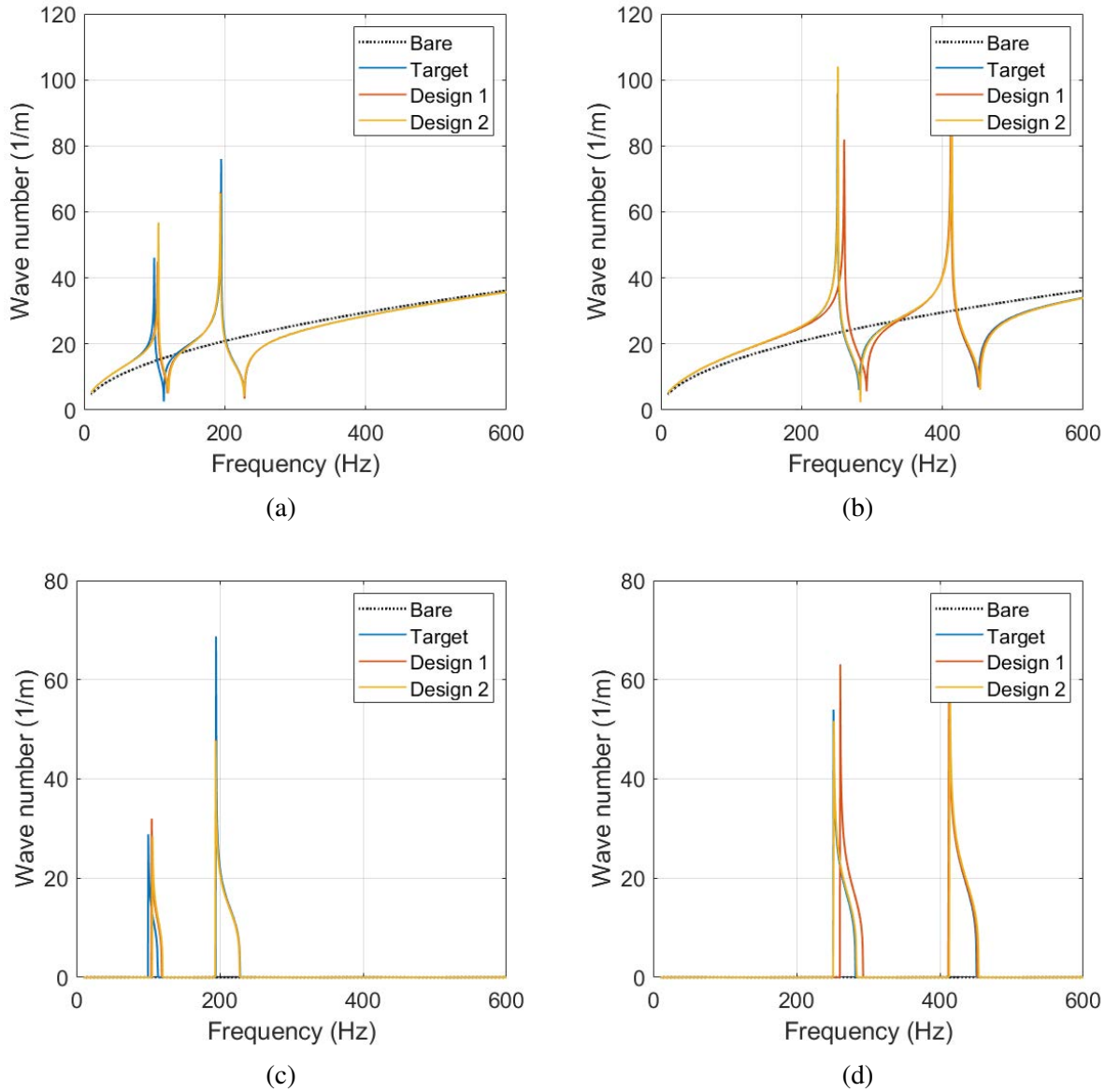

Figure 5: Dispersion curves (real and imaginary parts) for a LRM beam using both the ideal (target) and the automatically generated resonator designs. Solid and dashed lines respectively depict the properties of the beam with and without resonators. (a) First request, real part. (b) Second request, real part. (c) First request, imaginary part. (d) Second request, imaginary part.

//onlinelibrary.wiley.com/doi/abs/10.1002/adem.201800864https://onlinelibrary.wiley.com/doi/10.1002/adem.201800864

[2] N. Jiménez, O. Umnova, and J.-P. Groby, Eds., *Acoustic Waves in Periodic Structures,*

Metamaterials, and Porous Media, ser. Topics in Applied Physics. Cham: Springer, 2021. [Online]. Available: https://link.springer.com/10.1007/978-3-030-84300-7

[3] P. A. Deymier, Ed., *Acoustic Metamaterials and Phononic Crystals*, ser. Springer Series in Solid-State Sciences. Berlin, Heidelberg: Springer, 2013. [Online]. Available: https://link.springer.com/10.1007/978-3-642-31232-8

[4] C. Claeys, N. G. Rocha de Melo Filho, L. Van Belle, E. Deckers, and W. Desmet, "Design and validation of metamaterials for multiple structural stop bands in waveguides," *Extreme Mechanics Letters*, vol. 12, pp. 7–22, 4 2017.

[5] D. P. Kingma and M. Welling, "Auto-Encoding Variational Bayes," *2nd International Conference on Learning Representations, ICLR 2014 - Conference Track Proceedings*, 12 2013. [Online]. Available: https://arxiv.org/abs/1312.6114v11

[6] I. J. Goodfellow, J. Pouget-Abadie, M. Mirza, B. Xu, D. Warde-Farley, S. Ozair, A. Courville, and Y. Bengio, "Generative Adversarial Nets," *Advances in Neural Information Processing Systems*, vol. 27, 2014. [Online]. Available: http://www.github.com/goodfeli/adversarial

[7] R. Gómez-Bombarelli, J. N. Wei, D. Duvenaud, J. M. Hernández-Lobato, B. Sánchez-Lengeling, D. Sheberla, J. Aguilera-Iparraguirre, T. D. Hirzel, R. P. Adams, and A. Aspuru-Guzik, "Automatic Chemical Design Using a Data-Driven Continuous Representation of Molecules," *ACS Central Science*, vol. 4, no. 2, pp. 268–276, 2 2018. [Online]. Available: https://pubs.acs.org/doi/full/10.1021/acscentsci.7b00572

[8] L. Wang, Y. C. Chan, F. Ahmed, Z. Liu, P. Zhu, and W. Chen, "Deep generative modeling for mechanistic-based learning and design of metamaterial systems," *Computer Methods in Applied Mechanics and Engineering*, vol. 372, p. 113377, 12 2020.

[9] C. Gurbuz, F. Kronowetter, C. Dietz, M. Eser, J. Schmid, and S. Marburg, "Generative adversarial networks for the design of acoustic metamaterials," *The Journal of the Acoustical Society of America*, vol. 149, no. 2, p. 1162, 2 2021. [Online]. Available: https://asa.scitation.org/doi/abs/10.1121/10.0003501

[10] W. Ma, F. Cheng, and Y. Liu, "Deep-Learning-Enabled On-Demand Design of Chiral Metamaterials," *ACS Nano*, vol. 12, no. 6, pp. 6326–6334, 6 2018. [Online]. Available: https://pubs.acs.org/doi/full/10.1021/acsnano.8b03569

[11] Y. Pathak, K. S. Juneja, G. Varma, M. Ehara, and U. D. Priyakumar, "Deep learning enabled inorganic material generator," *Physical Chemistry Chemical Physics*, vol. 22, no. 46, pp. 26 935–26 943, 12 2020. [Online]. Available: https://pubs.rsc.org/en/content/articlehtml/2020/cp/d0cp03508dhttps://pubs.rsc.org/en/content/articlelanding/2020/cp/d0cp03508d

[12] A. Girard and N. Roy, *Structural Dynamics in Industry*. Wiley, 2008. [Online]. Available: https://onlinelibrary.wiley.com/doi/book/10.1002/9780470610916

[13] L. Liu and M. I. Hussein, "Wave motion in periodic flexural beams and characterization of the transition between bragg scattering and local resonance," *Journal of Applied Mechanics, Transactions ASME*, vol. 79, no. 1, 1 2012. [Online]. Available: https://asmedigitalcollection.asme.org/appliedmechanics/article/79/1/011003/475168/Wave-Motion-in-Periodic-Flexural-Beams-and

[14] K. Sohn, H. Lee, and X. Yan, "Learning Structured Output Representation using Deep Conditional Generative Models," *Advances in Neural Information Processing Systems*, vol. 28, 2015.

[15] L. Salamanca, A. A. Apolinarska, F. Pérez-Cruz, and M. Kohler, "Augmented Intelligence for Architectural Design with Conditional Autoencoders: Semiramis Case Study," *Towards Radical Regeneration*, pp. 108–121, 2023. [Online]. Available: https://link.springer.com/chapter/10.1007/978-3-031-13249-0_10

[16] *ANSYS Mechanical*, Release 22 ed. ANSYS, Inc.